2

BNL-NUREG-31796
CONF-820802--47

MASTER

TRANSIENT CORE-DEBRIS BED HEAT-REMOVAL EXPERIMENTS AND ANALYSIS

by

BNL-NUREG--31796
DE83 000712

T. Ginsberg, J. Klein, J. Klages, C. E. Schwarz;
J. C. Chen (Lehigh University)

Brookhaven National Laboratory
Department of Nuclear Energy
Experimental Modeling Group
Upton, NY 11973

August 1982

Presented at International Meeting on Thermal Nuclear Reactor Safety
August 29-September 2, 1982
Chicago, Illinois

TRANSIENT CORE-DEBRIS BED HEAT-REMOVAL EXPERIMENTS AND ANALYSIS

T. Ginsberg, J. Klein, C. E. Schwarz, J. Klages

Brookhaven National Laboratory
Department of Nuclear Energy
Upton, NY 11973

J. C. Chen

Lehigh University
Department of Chemical Engineering
Bethlehem, PA 18015

ABSTRACT

An experimental investigation is reported of the thermal interaction between superheated core debris and water during postulated light-water reactor degraded core accidents. Data are presented for the heat transfer characteristics of packed beds of 3 mm spheres which are cooled by overlying pools of water. Results of transient bed temperature and steam flow rate measurements are presented for bed heights in the range 218 mm-433 mm and initial particle bed temperatures between 530K and 972K. Results display a two-part sequential quench process. Initial frontal cooling leaves pockets or channels of unquenched spheres. Data suggest that heat transfer process is limited by a mechanism of countercurrent two-phase flow. An analytical model which combines a bed energy equation with either a quasi-steady version of the Lipinski debris bed model or a critical heat flux model reasonably well predicts the characteristic features of the bed quench process. Implications with respect to reactor safety are discussed.

INTRODUCTION

Analyses of core meltdown accidents in light water reactors are being performed to develop an understanding of the consequences of such postulated accidents [1]. Analysis of containment building pressurization as a result of loadings imposed by the core melt is an integral feature of these studies [2,3]. Two sources of containment pressurization of major concern are: (i) steam generation as a result of quenching (removal of stored energy) of hot core debris with cooling water and (ii) gas release resulting from decomposition of the concrete as a result of the thermal load imposed by the core melt.

Two models have been used to characterize the interaction between hot core debris and water. The MARCH code's "HOTDROP" model [4] assumes that the core debris is suspended in an infinite sea of water and that heat transfer is limited by the particle debris internal and external thermal resistances. Steam production is governed by the total surface area of the fragments. On the other hand, steady state debris bed cooling models have been used to predict the steam production rate resulting from quenching of packed beds of solid core debris. The validity of these models when applied to the transient cooling of debris beds has not been established by comparison with suitable transient quench experiments.

One prior investigation of transient quench characteristics of superheated debris beds has been reported [5], in which the beds were cooled by an overlying pool of water. Water was observed to penetrate at a constant rate into the bed while leaving pockets of dry spheres. The heat transfer characteristics of the quench process, however, were not quantified.

This paper presents the results of an experimental investigation whose objective is to provide an understanding of the thermal interaction between superheated core debris and water during postulated light-water reactor degraded core accidents. The experiment was designed to study the heat transfer characteristics of superheated spheres as they are quenched in a packed bed configuration by an overlying pool of water. A model based upon the experimental results is presented and implications with respect to reactor safety are discussed.

DESCRIPTION OF EXPERIMENT

In the experiment, packed beds of initially hot spheres were quenched by an overlying pool of water. Thermal-hydraulic measurements were obtained during the transient, constant-pressure quench process. The apparatus is shown in Figure 1.

Steel spheres were preheated in a stainless steel container positioned in the furnace. Hot air was used to obtain a uniform particle temperature distribution. A Nichrome wire heating system was used to preheat the test section wall to the required temperature prior to a run. While in the oven, the particles rested on a sliding shutter. The shutter plates could be retracted by air powered, spring-loaded pistons upon actuation by an electrical impulse.

The test vessel shown in Figure 1 is a Schedule 10 stainless steel pipe, 1.219 m long, 108.2 mm inside diameter, with a 3.05 mm wall thickness. It is closed at the bottom with a stainless steel flange which contains a drain port for removal of water and the spheres. A length of Pyrex glass pipe above the pipe permits visual observation of boiling in the pool of water above the particle bed. The test section is instrumented with thermocouples which penetrate through the wall into the test container. The thermocouple junctions are located at the center of the pipe. Thermocouples are also mounted on the outer wall of the pipe.

In addition to the interior "bed" and exterior wall thermocouples, a piezoelectric pressure transducer was mounted on the wall of the test section to monitor pressure fluctuations in the two-phase pool above the particle bed. This signal was used to identify the times of initiation and termination of boiling activity within the test vessel.

In the early stages of the work the steam was vented to the atmosphere via the steam vent shown in Figure 1. The apparatus was subsequently modified to incorporate the turbine flowmeter shown in Figure 1(b). This flowmeter was used to monitor the flow of steam during the particle quench process. In these latter experiments all of the piping which led to the flowmeter were preheated to the water saturation temperature prior to a run.

All instrument signals were sampled and recorded using a computer-controlled data acquisition system.

An experimental run was initiated after establishing the desired initial sphere, water and wall temperatures. At that time the shutter was retracted and the particles were dropped into the dry test vessel, where they formed a packed bed. After a short wait period, the water was released from the holding vessel onto the particle bed, initiating the quench process. Data acquisition continued until termination of boiling activity within the test vessel. Table I summarizes the range of experimental parameters considered in the study.

EXPERIMENTAL RESULTS

Temperature Traces and Frontal Propagation Data

A typical set of bed temperature traces is shown for Run No. 116 in Figure 2. The temperature traces are labeled by the thermocouple (TC) identification number. TC2 was located at the base of the bed. The remaining thermocouples were spaced in ascending order every 50 mm. TC8 was the uppermost thermocouple located 300 mm from the base of the bed. The key feature of Figure 2 is the sequence of step changes in temperature, beginning with TC8 located near the top of the bed. This sequence proceeded in the downward direction to each thermocouple in the bed. The temperature at each position suddenly fell from the initial sphere temperature to the liquid saturation temperature. Figure 2 also indicates that several of the thermocouples partially recovered their superheated temperatures subsequent to the first arrival of liquid. In this case four channels (TC Nos. 4, 6, 7, 8) exhibit this behavior. The temperature recovery characteristic of Run No. 116 occurred in many, though not all, of the experiments. These four thermocouples were finally quenched in a sequential pattern from the bottom upwards. A sequential pattern of wall quenching was also observed to proceed from the bottom upwards (not shown).

Three "frontal" particle bed cooling patterns are suggested by the bed and wall temperature traces. The times of arrival of each of the three cooling fronts are presented in Figure 3 as a function of axial position in the test column. Figure 3 shows the advance of a downward-propagating front which reaches the bottom of the bed at 165 seconds after initial water-bed contact. At this point an upward-propagating front is observed which is responsible for "final" cooling of the particle bed as well as the test wall.

Least squares analyses were performed on the frontal position data in order to obtain the apparent speeds of the initial downward propagating cooling front and the final upward quench front. The downward-propagating front advanced, in Run No. 116, at a speed v_d = 1.92 mm/s. The upward-propagating front advanced at a speed v_u = 0.98 mm/s. The results of all experiments indicate that v_d is greater than v_u.

The influence of initial particle temperature on the transient bed quench characteristics is displayed in terms of frontal propagation results in Figure 4. The sequential pattern of downward and upward cooling front progressions is observed for all the initial temperatures. The greater the initial bed temperature, however, the slower were the speeds of both the upward- and downward-propagating cooling fronts. As in Figure 3 the downward front advanced more rapidly than the upward front.

Figure 5 shows the effect of bed height on the frontal propagation data. These results suggest that the speeds of frontal propagation v_d and v_u are independent of bed height for fixed initial bed temperature. The effect of bed height is simply to delay the time of arrival of the downward cooling front to the base of the bed by times proportional to the differences in bed height.

Bed Heat Transfer Rates

Prior to installation of the turbine flowmeter system for the steam flowrate measurement, an estimate of th time-average bed heat transfer rate was made. The time period during which boiling was observed in the test vessel, Δt, was determined from the piezoelectric transducer traces. Together with the initial bed stored energy, the average bed heat flux for a set of conditions was computed as

$$q'' = \frac{mc\ (T_o - T_{SAT})}{A\ \Delta t} \qquad (1)$$

The results of these calculations are shown in Figure 6. They indicate that the time-average rate of heat transfer from the particles to the water was approximately 10^6 W/m^2 and independent of bed temperature for initial bed temperatures in the range 530 K to 970 K.

Steam Flow Rates

Figure 7 shows a representative trace of steam flow rate vs. time for Run No. 215. Also shown in Figure 7 is the time t_d that the thermocouple data indicated arrival of the downward-moving front to the base of the bed.

The first indication of flow in Figure 7 is attributable to closure of the shutter which isolates the oven from the system and hence forces the steam through the path to the turbine flowmeter. The initial contact between water and spheres is marked, in both cases, by the sharp rise in steam flowrate. Photographic observation in earlier tests using a Pyrex test vessel indicated that during approximately 10-15 seconds following the initial contact the upper portion of the bed was intermittently fluidized. The large initial flowrates were likely the result of this interaction. Following the initial interaction the steam flowrate remained, except for the observed fluctuations, reasonably steady for the duration of the bed quench process. The average steam flowrate during this period is approximately $\dot{Q}_v = 0.00597$ m^3/s, (±13%). Assuming that this flowrate is representative of the rate of heat transfer between water and particles, the bed heat removal rate can be computed from the relationship

$$q'' = \frac{\dot{Q}_v}{A} h_{fg} \rho_v \qquad (2)$$

For the conditions of Run No. 215, the bed heat removal flux is $q'' = 0.88 \times 10^6$ (±13%) W/m^2. This is in close agreement with the average heat flux data presented in Figure 6.

The results shown in Figure 7 indicate no detectable difference in steam generation rate during the time of passage of the downward front (to t_d) and the upward front (times greater than t_d). If the steam flowrate is assumed constant for the entire time period of the quench process then the fraction of energy, f_d, removed from the bed during passage of the downward front is

$$f_d = \frac{\Delta t_d}{\Delta t} \qquad (3)$$

The results of Figure 7 indicate that on this basis, $f_d = 0.4$. Approximately 40% of the stored energy is removed during passage of the downward-progressing cooling front. The remaining stored energy is then removed during the passage of the upward front. Additional data taken prior to installation of the turbine meter suggest that f_d = 0.30-0.40 over the initial particle temperature range of Table I.

Frontal Progression Speeds

The frontal progression speeds v_d and v_u were obtained from the frontal propagation data for each set of experimental conditions. These data, calculated using a linear least squares analysis, are shown in Figure 8. Data from Armstrong, et al [5] are also presented. The results indicate that the frontal speeds decrease with increasing temperature and that the downward frontal speed is consistently larger than the corresponding upward frontal speed.

ANALYSIS

Summary of Experimental Observations

The experimental data suggest that packed beds of superheated particles which were cooled by water supplied from overlying pools of water were quenched in a two-stage cooling process. Water initially penetrated the beds during the initial downward frontal progression. This process was irregular and left channels or pockets of dry particles. This observation agrees with those of Armstrong, et al [5]. It is estimated that approximately 30-40% of the initial stored energy was transferred to the water during this time period. A final upward-directed cooling front began its progression subsequent to completion of the downward process. During this final upward frontal progression the remaining stored energy was removed from the particles.

The results further indicate that the rate of heat transfer from the particle bed to water is independent of the mass of particles and initial particle bed temperature. The time required to quench the bed, however, increases with particle mass and initial particle temperature. The speeds of the two cooling fronts decrease with increasing initial particle temperature. The initial water penetration rate, v_d, is greater than the speed of the upward final quench front. Finally, the turbine flowmeter data show that the steam flowrate was nearly constant for the entire duration of the quench process, inclusive of both frontal progression periods. This is taken to imply that the rate of heat transfer from the bed to the water was limited by processes common to both frontal periods.

Basic Model Assumptions

Based upon the above observations it is assumed that the packed bed heat transfer occurred at the quench front during both the downward and upward frontal periods. The rate of heat transfer with liquid supplied from an overlying pool is assumed to be limited by maximum rate at which vapor can be removed from the bed under conditions of countercurrent two-phase vapor-liquid flow in or to the packed bed.

Consider the schematic representation of the packed bed shown in Figure 9. Assume that the bed is initially dry and at temperature T_o. Both frontal processes are treated one-dimensionally (averaged radially). The downward-moving front penetrates axially at speed v_d, while at the same time leaving pockets or channels of unquenched particles. It is assumed that a fraction f_d of the particle bed is quenched, i.e., its temperature is reduced to T_{SAT}, during passage of this initial front. The bed temperature for $z < z^*$ remains at $T = T_o$ until passage of the front.

The final upward frontal period is also treated one-dimensionally. The region beneath the front, $z < z^*$, is uniformly at temperature T_{SAT}. The speed of the front is v_u and the remaining fraction of the bed interval energy, $1-f_d$, is transported to the water during this time period.

Particle Bed Energy Equations

Consider, first, the downward-propagating frontal period. A generalized conduction equation for the bed may be written as

$$\rho c\,(1-\varepsilon)\,\frac{\partial T}{\partial t} = \nabla \cdot \nabla \vec{q} \qquad (4)$$

Assume, for the moment, that the entire region $z > z^*$ is quenched and at temperature T_{SAT} and the entire region below z^* is at initial temperature T_o. Equation (4) is integrated across the entire volume of the bed. The result, using Leibnitz's rule,

is the frontal propagation equation

$$\rho c\ (1-\varepsilon)\ (T_o-T_{SAT})\ \frac{dz^*}{dt} = -\ \frac{Q_d}{A} \tag{5}$$

where Q_d/A is the bed heat removal rate. It is further assumed, as discussed above, that only a fraction f_d of the bed stored energy is removed. In addition the quantity ρc, representing the heat capacity of the bed particulate is modified to account for the additional heat capacity of the test vessel wall in the experiments. The resulting downward frontal propagation equation is

$$v_d\ f_d\ (\rho c)_{eff}\ (1-\varepsilon)\ (T_o-T_{SAT}) = -\ Q_d/A = -q''_d \tag{6}$$

Following an analogous procedure, the corresponding equation for upward frontal propagation is

$$v_u\ f_u\ (\rho c)_{eff}\ (1-\varepsilon)\ (T_o-T_{SAT}) = -\ Q_u/A = -q''_u \tag{7}$$

Particle Bed Heat Removal Rate

Assume that the particle bed stored energy is removed from the bed as the latent heat of vaporization of water. In addition, assume that the heat removal rates Q_d and Q_u are equal, as suggested by the experimental results. The heat removal rate is assumed to be limited by the maximum rate at which vapor can be removed from the bed under gravity-driven countercurrent two-phase flow conditions.

Three models are considered for the maximum countercurrent flow vapor flux:

(i) Rayleigh-Taylor Instability Critical Heat Flux (CHF) Model
(ii) Quasi-Steady Lipinski Debris Bed Model
(iii) Quasi-Steady Ostenson Debris Bed Model.

These are discussed in turn below.

(i) CHF Model

It has been suggested [6] that, for large particle diameter, the vapor flux from an internally heated packed bed is limited by the countercurrent vapor-liquid mechanisms existing above the bed. The model for critical heat flux (CHF) from a flat plate, developed by Zuber [7] to characterize the Rayleigh-Taylor instability mechanisms under these conditions, is used to compute the bed heat removal rate under the transient quench conditions of the experiments reported here.

(ii) Quasi-Steady Lipinski Model

Lipinski [8] has developed a model for the maximum rate of heat removal from internally-heated packed beds under steady state conditions. This model is a separated flow treatment of two-phase flow in a packed bed and employs a generalized D'Arcy's law representation for the fluid-solid flow resistances. The model, which does not consider vapor-liquid momentum transfer, has been found useful in correlating maximum steady state bed heat removal data.

Lipinski's treatment of the momentum interactions are applied to the slow transient quench conditions of the experiment reported here. Equations (3.1) and (3.2) of Reference 8 are used as the applicable momentum balances. The total mass balance equation, however, is modified to account for the liquid flux into the bed which fills the void space within the bed during the quench process. Separated flow continuity equations for the vapor and liquid may be written, integrated across the two-phase portion

of the bed and are then added to give the following mass balance equations

$$\rho_u V_v + \rho_\ell V_\ell = \begin{cases} (1-\alpha)\ \rho_\ell v_d \\ \alpha\ \rho_\ell\ v_u \end{cases} \tag{8}$$

for the two frontal periods. These equations replace Lipinski's Equation (3.4) of Reference 8.

The above mass balance equation is then combined with the remainder of Lipinski's debris bed model to give the following equation for V_v, the vapor flux at the top of the bed:

$$\left(\frac{1}{\rho_v\ \eta_v} + \frac{1}{\rho_\ell\ \eta_\ell}\right) \frac{\rho_v^2\ V_v^2}{\eta} + \left(\frac{\nu_v}{\kappa_v} - \frac{2B\kappa}{\eta\eta_\ell} + \frac{\nu_\ell}{\kappa_\ell}\right) \frac{\rho_v\ V_v}{\kappa}$$

$$+ \frac{\rho_\ell}{\eta\eta_\ell}\ B^2 - \frac{\mu_\ell B}{\kappa\kappa_\ell} - (\rho_\ell - \rho_v)\ g \left(1 + \frac{\lambda_c}{H}\right) = 0 \tag{9}$$

where

$$B = \begin{cases} (1-\alpha)\ v_d & \text{(downward front)} \\ \alpha\ v_u & \text{(upward front)} \end{cases} \tag{10}$$

and λ_c is the "capillary force length" defined by Lipinski. Equation (9) replaces Lipinski's Equation (3.35).

Equation (9) may be solved for V_v as a function of void fraction (which is included implicitly in the relative permeabilities as well as explicitly in the definition of B). The bed heat removal rates are then computed from V_v

$$q'' = \frac{Q}{A} = \rho_v\ h_{fg}\ V_v \tag{11}$$

as a function of α for both the downward and upward frontal periods. The maximum rate of heat removal is then obtained by maximizing q" with respect to void fraction.

(iii) Quasi-Steady Ostenson Model

Ostenson [9] proposed a bed maximum heat flux model based upon a two-phase flow flooding correlation for application to packed beds of large particles. While the basis of the model derives from two two-phase flow in circular pipes with no particles present, the empirical constant was obtained from experiments with packed towers in the chemical processing industry. This model was used in the context of the experiment reported here. It was, however, modified in a manner analogous to that described above in the discussion of the Lipinski model. Equation (8) above was used to replace Ostenson's continuity equation. A solution was then obtained for the vapor flux and

the heat flux was computed using Equation (11) for both q_d and q_u.

Solution

The characteristics of the particle bed quench process may be calculated by solving Equations (6), (7) and (8) together with one of the bed heat removal models discussed above. In addition, however, the quantity f_d must be specified. The available data for particle temperatures up to 970K suggest that f_d = 0.30-0.40.

DISCUSSION

Calculations based upon the analytical model presented above are compared with the experimental heat transfer data in Figure 7 and with the experimental propagation data in Figure 8. Results are presented for f_d = 0.40.

Figure 7 indicates that bed heat transfer rate is predicted reasonably well by either the Zuber CHF model or the quasi-steady Lipinski debris bed model (labeled "TRANSBED"). The CHF model predicts no effect on bed temperature. It is a purely hydrodynamic model based upon Rayleigh-Taylor instability at the bed surface. In applying this model it is assumed that the bed surface is equivalent to a flat plate. The debris bed model, which was modified to account for the transient continuity aspect of the quench process, predicts a weak dependence on bed temperature. It is not possible to conclude from this data whether the bed quench process is limited by Rayleigh-Taylor instability above the bed surface, or by countercurrent two-phase flow flooding within the bed. The Ostenson model, which is an empirical countercurrent flow relationship and does not explicitly consider the balance of forces within the packed bed, underestimates the bed heat transfer rate. While the TRANSBED model somewhat overestimates the data, it provides better agreement with the data of this experiment. Finally, it is noted that the transient aspects of the quench process can be neglected for bed temperature differences greater than approximately 400K, insofar as bed heat transfer rate is concerned. This is definitely not the case, however, for the behavior of the frontal speed.

Data for the frontal speeds are shown in Figure 8 together with the transient bed quench model prediction using the TRANSBED model. Downward frontal traverse speed data from Reference 5 are presented along with those of the experiments reported here. (The differences in bed depth are negligible in terms of model predictions). Agreement of the cooling front data with the analytical model proposed here is favorable over the entire range of bed temperatures from approximately 180K to 970K. The only possible exception is at the lowest bed temperature where the data scatter is rather large.

The data shown in Figure 8 represent experimental results using particle beds of 3 mm stainless steel spheres. The data cover a range of bed height from 200 mm to 750 mm and an initial bed temperature range of 180K to 970K.

The favorable agreement of the model with the data over the range of conditions outlined above lends credence to the interpretation of the results characterized in the analysis section of this paper. The conclusions which are drawn from the experimental results, data analysis and analytical modeling are presented below.

SUMMARY AND CONCLUSIONS

Experimental data are presented which characterize the transient quench characterisitcs of packed beds of superheated spheres which were cooled by vaporizing liquid supplied from an overlying pool of water. The particle size in the experiments was 3 mm. Data are presented for bed heights in the range 200 mm-750 mm and in the bed temperature difference (T_o-T_{SAT}) range 180K-970K. An analytical model of the transient quench process is presented and predictions based on the model are compared

with the bed heat transfer rate and frontal propagation speed data. The model contains one free parameter which is estimated from available data. Agreement between the data and the model predictions are favorable over the range of conditions for which data are available. The following conclusions are drawn from the study reported here:

- A superheated particle bed quenches in a two-step bi-frontal process. A partial quench front first propgates downward removing a fraction (f_d) of the stored sensible heat of the bed. A second upward-directed quench front starts when the downfront reaches the bed bottom. The upward front removes the balance ($1-f_d$) of the stored energy. Experimental data suggest that $f_d = 0.3-0.4$.

- The net rate of energy removal from the bed is, within the scatter of the data, independent of initial bed temperature and is identical during both the downward and upward frontal periods.

- The above observations strongly suggest that the phenomenon which limits the net heat removal from a superheated bed is hydrodynamic in nature. This is consistent with the hypothesis that the heat transfer is limited by the hydrodynamics of countercurrent two-phase flow, either just above the bed or within the bed.

- A transient bed quench model is presented. One-dimensional bed energy equations were solved simultaneously with three hydrodynamic models for the limiting volume flux of vapor.

  Predictions based upon both the Lipinski [8] debris bed model and the Rayleigh-Taylor CHF model [7]. both provide favorable agreement with the available bed heat transfer rate data. They also lead to good predictions of the cooling front propagation rate data.

- Calculations for larger particle sizes indicate that the Lipinski and Rayleigh-Taylor models provide divergent predictions. Data for larger particle sizes are needed to establish the validity of either model over an extended range.

IMPLICATIONS

The results of the investigation suggest that the rate of containment building pressurization resulting from quenching of superheated beds of core debris by overlying pools of liquid would be limited by the hydrodynamics of countercurrent two phase flow to or within the beds. The data and models indicate that this conclusion is independent of initial bed temperature.

The observed frontal characteristics, however, suggest that the debris ahead of the initial cooling front would remain dry until arrival of the downward front. Attack of the concrete by the hot solid debris must be considered during this time period.

NOMENCLATURE

A	bed cross-sectional area
c	specific heat
f	fraction of bed energy removal
g	gravitational acceleration
h_{fg}	latent heat of vaporization
H	bed height
m	mass of particles
q''	bed heat removal flux
$\vec{q}$	bed heat flux vector
Q	bed heat removal rate
$\dot{Q}_v$	rate of steam production
t	time
T	bed temperature
T_o	initial bed temperature
v	bed frontal propagation speed
V	superficial velocity
z	axial coordinate
z^*	frontal position coordinate (moving)

α	vapor volume (void) fraction
ε	bed porosity
η	bed "passability"
η_ℓ η_v	specific passability
κ	bed permeability
κ_ℓ κ_v	specific permeability
λc	"capillary force length"
μ	viscosity
ν	kinematic viscosity
ρ	density

Subscripts

d	downward front
eff	effective
ℓ	liquid
SAT	saturation condition
u	upward front
v	vapor

ACKNOWLEDGEMENTS

This work was performed under the auspices of the United States Nuclear Regulatory Commission, Office of Nuclear Regulatory Research, Division of Severe Accident Evaluation.

The authors acknowledge the help of Ms. Linda Hanlon in preparation of this manuscript for publication.

REFERENCES

1. Meyer, J. F., "Preliminary Assessment of Core Melt Accidents at the Zion and Indian Point Nuclear Power Plants and Strategies for Mitigating Their Effects," Vol. 1, U. S. Nuclear Regulatory Commission Report, NUREG-0850 (November 1981).

2. Yang, J. W., "Cooling of Core Debris and the Impact on Containment Pressure," Brookhaven National Laboratory, NUREG/CR-2066 (July 1981).

3. Pratt, W. T. and R. A. Bari, "Containment Response During Degraded Core Accidents Initiated by Transients and Small Break LOCA in the Zion/Indian Point Reactor Plants," Brookhaven National Laboratory, BNL-NUREG-51415 (July 1981).

4. Wooton, R. O. and H. I. Avci, "MARCH (Meltdown Accident Response Characteristics) Code Description and User's Manual," Battelle Columbus Laboratories, NUREG/CR-1711 (October 1980).

5. Armstrong, D. R., D. H. Cho and L. Bova, "Formation of Dry Pockets During Penetration into a Hot Particle Bed," Trans. Am. Nucl. Soc., 41, 418-419 (June 1982).

6. Squarer, D., A. T. Pieczynski and L. E. Hochreiter, "Effect of Debris Bed Pressure, Particle Size and Distribution on Degraded Reactor Core Coolability," Nucl. Sci. and Eng. 80, 2-13 (1982).

7. Zuber, N., "Hydrodynamic Aspects of Boiling," Dissertation, Univ. of California, AECU-4439 (1959).

8. Lipinski, R., et al., "Advanced Reactor Safety Research Quarterly Report January-March 1980," Sandia National Laboratories, NUREG/CR-1594, 13, 1, 88 (April 1981).

9. Ostenson, R. W. and R. J. Lipinski, "A Particle Bed Dryout Model Based on Flooding," Nuc. Sci. & Eng., 79, 110-113 (1981).

TABLE I

Test Parameter Ranges

Packed Bed Particles	3 mm (± 0.25 mm) spheres
Particle Material	302 stainless steel
Bed Diameter	108.2 mm (test vessel i.d.)
Mass Particles	10 - 20 kg
Mass Water	8 -14 kg
Particle Temperature	533K - 972K (500F-1300F)
Water Temperature	274K - 360K
Particle Bed Height	218 - 433 mm
Pressure	0.1 MPa (1 bar)
Bed Porosity	0.37 - 0.41 (separate tests)

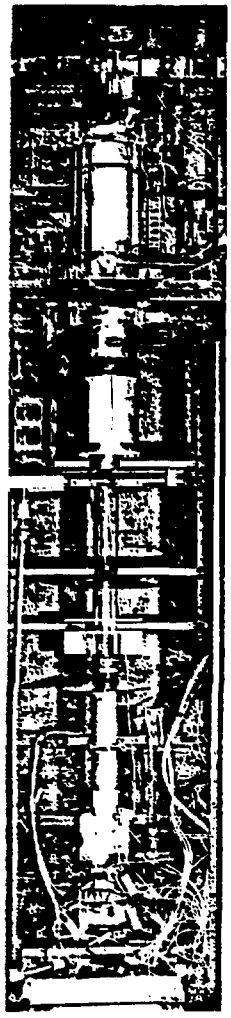

(a)

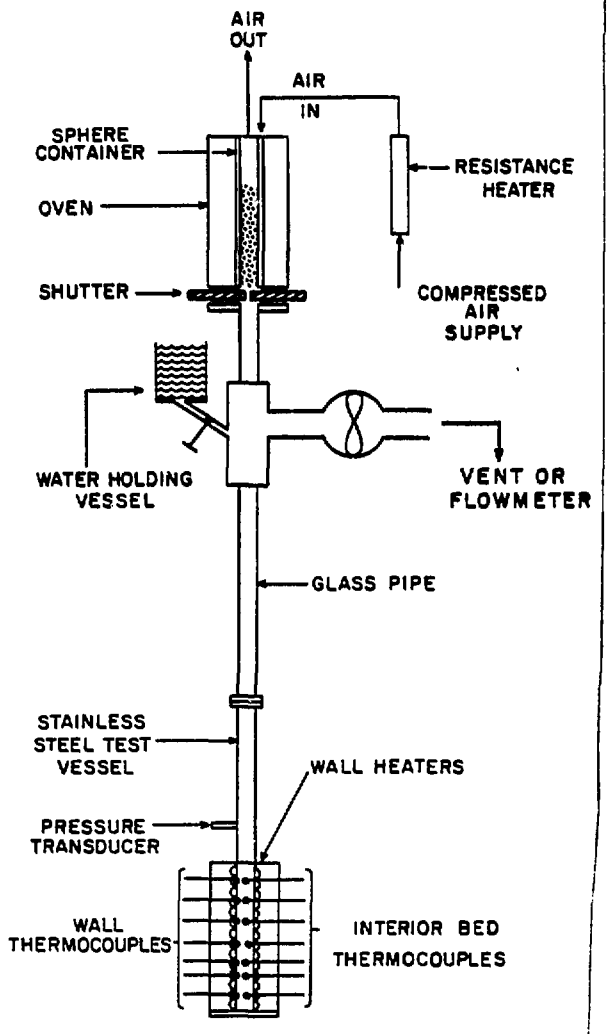

(b)

FIGURE 1-(a) Photograph and (b) Schematic Diagram of Test Apparatus

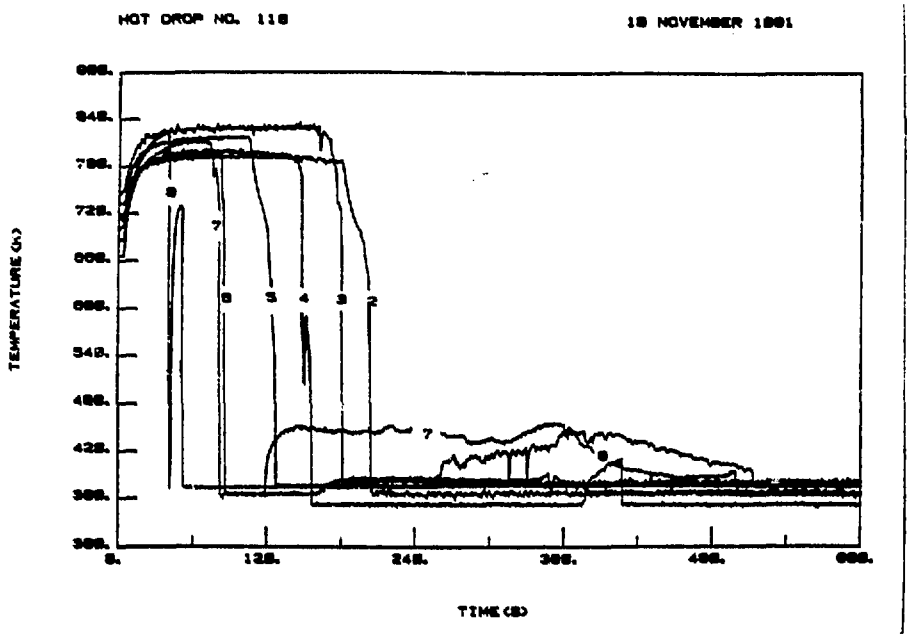

FIGURE 2 - Bed Temperature Traces: T_o=800K; Bed Height=327 mm

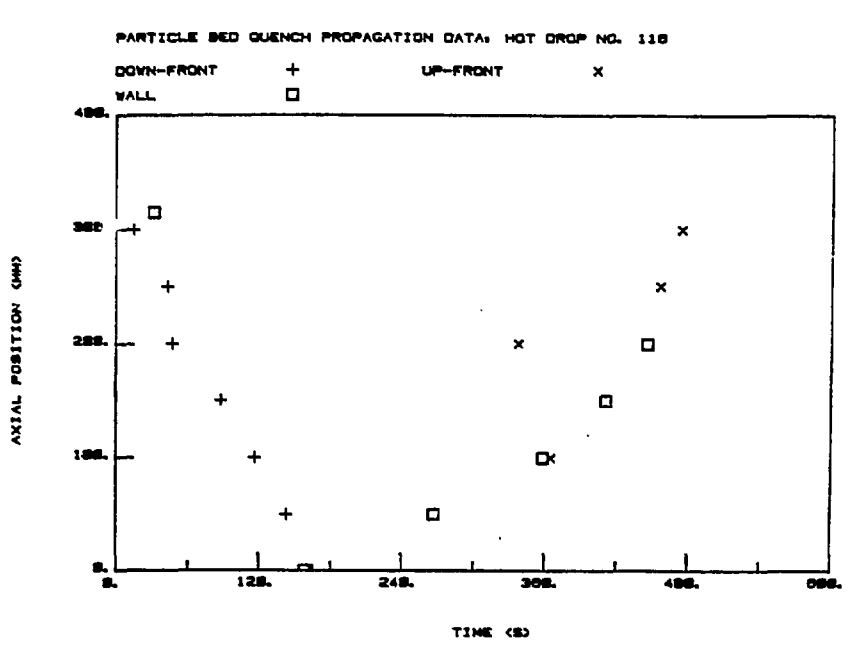

FIGURE 3 - Frontal Propagation Results: T_o=800K; Bed Height=327 mm

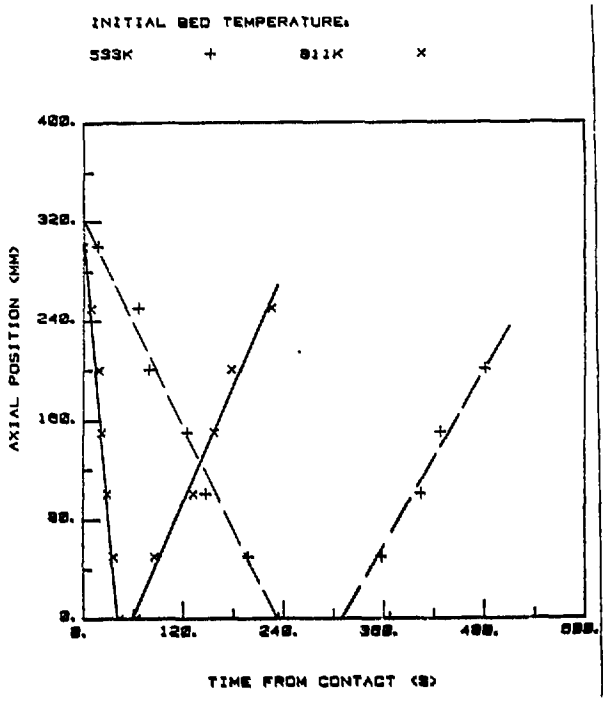

FIGURE 4-Effect of Bed Temperature on Frontal Propagation: H=327 mm

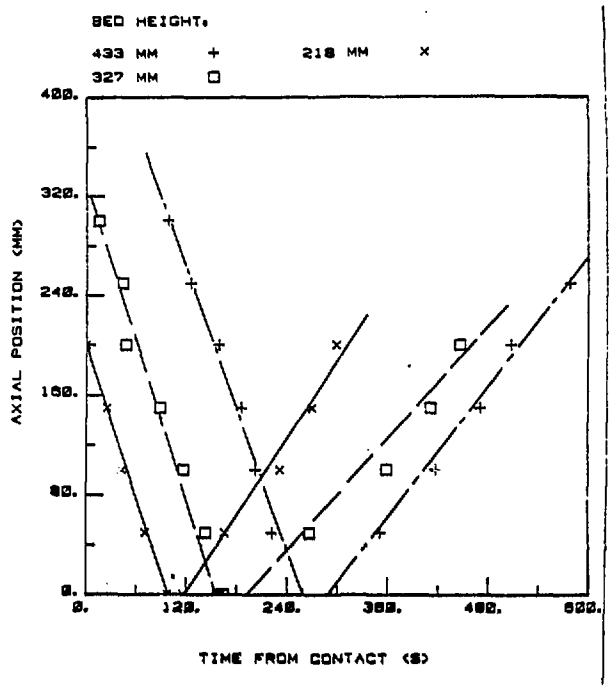

FIGURE 5-Effect of Bed Height on Frontal Propagation: T_o=800K

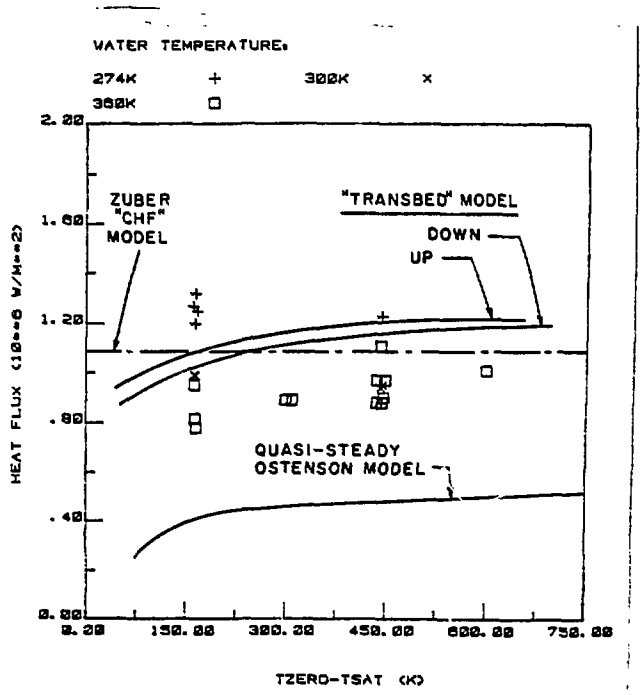

FIGURE 6-Particle Bed Heat Transfer Rate: Measured and Calculated

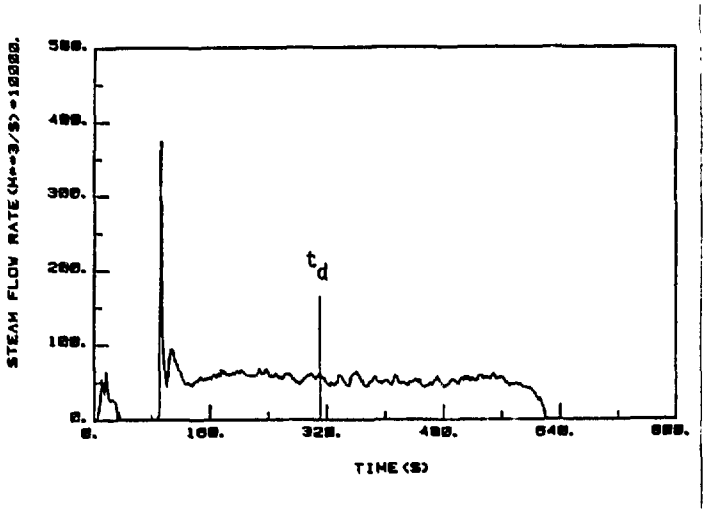

FIGURE 7-Steam Flow Rate Measurement: H=327 mm; T_o=800K

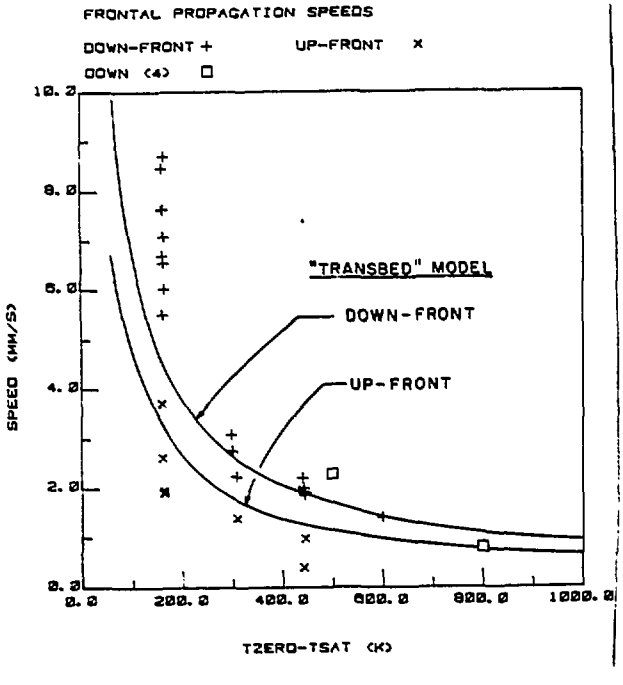

FIGURE 8-Frontal Progression Speeds

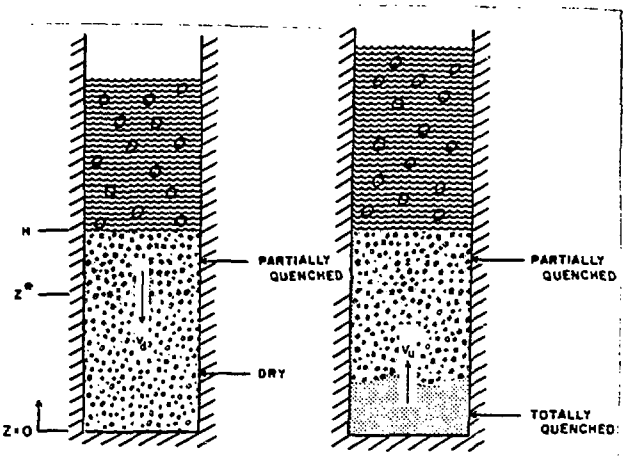

FIGURE 9-Schematic Representation of Bed Quench